



Magnetic effects on fundamental modes in rotating neutron stars with a purely toroidal magnetic field

Anson Ka Long Yip ^{1,*} and Tjonnie Guang Feng Li ^{2,3}

¹*Department of Physics, The Chinese University of Hong Kong, Shatin, N.T., Hong Kong*

²*Institute for Theoretical Physics, KU Leuven, Celestijnenlaan 200D, B-3001 Leuven, Belgium*

³*Department of Electrical Engineering (ESAT), KU Leuven,
Kasteelpark Arenberg 10, B-3001 Leuven, Belgium*

(Dated: September 15, 2025)

Electromagnetic and gravitational-wave signals from neutron stars are shaped by rapid rotation and strong magnetic fields. Determining these properties is essential to interpret such signals, but current measurements are limited: rotation estimates rely on electromagnetic detections and assume uniform rotation, while inferring interior magnetic fields remains ambiguous due to a lack of direct observations. Measuring the excited fundamental modes of neutron stars in gravitational-wave signals offers a promising solution, as these modes encode information about stellar composition, structure, and dynamics. Previous studies have examined the individual effects of rotation and magnetic fields on these modes, identifying magnetic suppression and establishing linear relations for the frequencies of the fundamental $l = 0$ quasi-radial mode f_F and $l = 2$ quadrupolar mode f_{2f} . However, few have investigated the combined influence of rotation and magnetic fields. Here, for the first time, we consider both rotation and a toroidal magnetic field to construct linear relations for quantifying f_F and f_{2f} , showing that their combined effects can be constrained by detecting these modes. Using 2D axisymmetric simulations, we demonstrate that quasi-linear relations between f_F , f_{2f} , stellar compactness M/R , and kinetic-to-binding energy ratio $T/|W|$ persist even with a toroidal magnetic field. The slope of these relations depends on the toroidal magnetization constant K_m . Additionally, measuring the frequency ratio f_{2f}/f_F enables inference of $T/|W|$ and the maximum magnetic field strength B_{\max} . Lastly, we show that differential rotation causes only minor deviations from predictions for uniform rotation. Thus, this work demonstrates that rotational and magnetic properties of neutron stars can be inferred from their fundamental modes.

I. INTRODUCTION

Neutron stars exhibit a wide range of rotation periods P , spanning from a few ms to several s. For example, classical pulsars generally rotate more slowly, with periods of $P \sim 16$ ms to several s. In contrast, millisecond pulsars are significantly faster, with $P \sim 1.55$ ms to a few ms. These rapid rotation rates result from the conservation of angular momentum during the collapse of their progenitor stars. As the stellar core contracts, angular momentum is redistributed, causing the newly formed neutron star to "spin up." Furthermore, it is believed that millisecond pulsars achieve these extreme rotation speeds through a spin-up process driven by the accretion of matter and angular momentum from a companion star in a binary system (see e.g. [1] for a review).

The measurement of neutron star rotation is primarily based on electromagnetic observations. For instance, the precise timing of their pulsed emissions allows for an accurate determination of P . However, there are astrophysical scenarios in which no electromagnetic counterpart is observed, such as the binary neutron star merger event GW190425 [2]. Additionally, this method of quantifying rotation by P applies only to cases of rigid rotation. In astrophysical events like core-collapse supernovae and binary neutron star mergers, neutron stars are expected to

exhibit differential rotation (see e.g. [3–5] for reviews).

Neutron stars are also known to host the strongest magnetic fields in the Universe, with field strengths reaching up to 10^{14-15} G. Highly magnetized neutron stars, such as magnetars, are believed to explain several enigmatic astrophysical phenomena, including soft gamma-ray repeaters and anomalous X-ray pulsars [6–10]. Moreover, magnetic fields can deform neutron stars, with the type of deformation depending on the field geometry. A purely toroidal magnetic field induces prolateness [11–13], whereas a purely poloidal field causes oblateness [14–16]. These deformations make rotating neutron stars potential sources of detectable continuous gravitational waves [17]. However, the true geometry of magnetic fields inside neutron stars remains uncertain. Stability analyses suggest that simple field configurations are prone to instabilities [18–22]. Magnetohydrodynamic (MHD) simulations propose that a mixed toroidal-poloidal configuration, known as a "twisted torus," is the most favorable [23–25]. Nevertheless, recent studies (e.g. [26]) suggest that instabilities may still persist in these mixed-field configurations.

Since the magnetic field governs neutron star emissions, understanding its configuration is critical. Surface magnetic field strengths are often estimated using the dipole spin-down model with radio observations [27, 28]. Recently, the Neutron Star Interior Composition Explorer (NICER) has enabled the deduction of the geometry and strength of surface magnetic fields from

* kalongyip@cuhk.edu.hk

X-ray emitting hotspots in pulsars [29, 30]. However, these methods only provide information about surface fields, leaving the internal magnetic field largely unexplored. Determining the geometry and strength of magnetic fields inside neutron stars remains a significant challenge.

Gravitational wave detections offer a novel way to probe the internal properties of neutron stars. The first detected signal, GW170817, originated from a binary neutron star merger [31]. Beyond mergers, violent astrophysical events like core-collapse supernovae and accretion-induced collapse could also excite oscillation modes in neutron stars, which are potential sources of detectable gravitational waves (see e.g. [32, 33]). These oscillation modes are strongly tied to the composition, structure and dynamics of the stars, making their detection a valuable tool for studying neutron star interiors. As mentioned, neutron stars are expected to possess both rapid rotation and strong magnetic fields, especially in these violent events that excite the oscillation modes. For example, a magnetic field strength as high as 10^{17-18} G could even be reached in proto-neutron stars formed right after core-collapse supernovae [34] and rotate with a period of $P \sim \mathcal{O}(1)$ ms [35]. Furthermore, binary neutron star merger simulations have demonstrated that the local maximum magnetic field can be amplified to $\sim 10^{17}$ G during the merger [36–39] and the hypermassive neutron stars formed from the mergers have a typical angular velocity of kHz (roughly corresponds to $P \sim \mathcal{O}(1)$ ms) [40]. Thus, understanding the effects of rotation and magnetic fields on oscillation modes is essential for probing the internal properties of neutron stars in these events.

The oscillation modes of rotating neutron stars have been extensively studied using perturbative calculations and dynamical simulations [32, 41–54]. In particular, [32] used dynamical simulations in the Cowling approximation (fixing spacetime while evolving matter equations) to study axisymmetric oscillation modes of uniformly and differentially rotating neutron stars and constructed linear relations for predicting the fundamental $l = 0$ quasi-radial mode frequency f_F and the fundamental $l = 2$ quadrupolar mode frequency f_{2f} as functions of the ratio of kinetic energy to gravitational binding energy $T/|W|$. Recently, our previous work [54] updated these linear relations by including both various degrees of differential rotation and dynamical spacetime for the first time. Hence, by measuring the fundamental mode frequency, we can infer the rotation of neutron stars, quantified by $T/|W|$, even in cases with differential rotation.

Similarly, oscillations in magnetized neutron stars have been studied using both Newtonian (e.g. [55]) and general relativistic approaches (e.g. [56–58]). Specifically, through dynamical simulations, our previous work [59] examined the axisymmetric oscillation modes of magnetized neutron stars with a purely toroidal field in dynamical spacetime and demonstrated the magnetic suppression effect on oscillation mode frequencies due to a strong toroidal field of $\sim 10^{17}$ G for the first time. Moreover,

by dynamically simulating the gravitational collapse of a magnetized neutron star due to a phase transition (typically known as phase-transition-induced collapse) for the first time [60], we showed that the internal magnetic field strength of a neutron star can be directly constrained by measuring the frequency of excited fundamental modes in the corresponding gravitational wave signals generated during the collapse [61].

Although the oscillations of rotating and magnetized neutron stars have been extensively studied individually, limited research has explored the combined effects of rapid rotation and strong magnetic fields. For instance, the oscillations of rotating magnetized neutron stars with purely toroidal magnetic fields [62] and purely poloidal magnetic fields [63] have only been studied using a Newtonian framework. However, this Newtonian approach is likely to introduce significant errors in determining the frequencies of oscillation modes. A study that incorporates both rotation and magnetic fields in dynamical spacetime is essential for improving our understanding of neutron star oscillations across different astrophysical scenarios.

To address this limitation, a promising approach would involve dynamical simulations capable of efficiently exploring a wide range of magnetized and rotating stellar models within a reasonable timeframe and with minimal computational resources. **Gmunu** [64–66], a new general-relativistic magnetohydrodynamics code, is well-suited for this purpose. It supports simulations in multiple dimensions (1D, 2D, and 3D) and coordinate systems (cartesian, cylindrical, and spherical) through a block-based adaptive mesh refinement (AMR) module, enabling the imposition of symmetries to reduce dimensionality and significantly lower computational costs for various problems. This flexibility enables users to choose the optimal dimensionality and coordinate system for their specific problem, and to impose symmetries that can further lower computational requirements when appropriate. The 2D axisymmetric simulations conducted in this study are particularly well-suited for investigating axisymmetric ($m = 0$) oscillation modes, such as the F -mode and 2f -mode studied by [32, 49, 54]. However, it should be emphasized that non-axisymmetric modes, including the $m = 1$ and $m = 2$ modes, may develop and play an important role during violent astrophysical events, such as binary neutron star mergers and core-collapse supernovae (see e.g. [67]). Therefore, by adopting 2D axisymmetry, this study is unable to capture such non-axisymmetric modes. A comprehensive investigation of these modes would necessitate fully 3D simulations without imposing axisymmetry. Additionally, **Gmunu** solves the elliptic metric equations under the conformally flat condition (CFC) approximation efficiently and robustly using the multigrid method. These capabilities make **Gmunu** an excellent tool for studying neutron star problems involving rapid rotation and strong magnetic fields [54, 59–61, 68–74].

In this work, for the first time, we account for both

rotation and magnetic fields to investigate how the magnetic suppression effect on the fundamental mode frequency, identified in our previous work [75], influences the linear relations quantifying f_F and f_{2f} as we presented in [54]. Specifically, we begin by constructing initial rotating neutron star models with a purely toroidal magnetic field using the open-source code **XNS** [34, 76–79]. These equilibrium models are then perturbed and evolved in dynamical spacetime using **Gmunu**. The details of the initial neutron star models and their evolution are provided in Section II. Next, in Sections III and IV, we investigate how the fundamental mode frequencies vary with the stellar compactness M/R and the kinetic-to-binding energy ratio $T/|W|$ of neutron stars respectively. Following this, we demonstrate that measuring the frequency ratio between the two fundamental modes f_{2f}/f_F can provide information about \mathcal{B}_{\max} and the kinetic energy-to-binding ratio $T/|W|$ in Section V. After that, we examine the deviations in the frequencies of the fundamental mode caused by differential rotation in Section VI, comparing them to the predictions derived from linear relations for uniformly rotating models. Finally, the conclusions of this study are presented in Section VII.

Unless otherwise specified, we choose dimensionless units for the physical quantities by setting the speed of light, the gravitational constant, and the solar mass to one, $c = G = M_\odot = 1$.

II. NUMERICAL METHODS

A. Initial neutron star models

We construct equilibrium models of rotating neutron stars with a purely toroidal magnetic field in axisymmetry using the open-source code **XNS** [34, 76–79]. These models are used as initial data for our dynamical simulations.

A polytropic equation of state is adopted to compute initial neutron star models,

$$P = K\rho^\gamma, \quad (1)$$

where P denotes the pressure, ρ denotes the rest-mass density and we choose the polytropic constant $K = 100$ and polytropic index $\gamma = 2$.

We assign the specific internal energy ϵ on the initial time-slice using,

$$\epsilon = \frac{K}{\gamma - 1} \rho^{\gamma-1}. \quad (2)$$

A magnetic polytropic law is used to model the toroidal magnetic field *enclosed in the star*,

$$\mathcal{B}_\phi = \alpha^{-1} K_m (\rho h \varpi^2)^m, \quad (3)$$

where α is the lapse function, K_m is the toroidal magnetization constant, h is the specific enthalpy, $\varpi^2 =$

$\alpha^2 \psi^4 r^2 \sin^2 \theta$, ψ is the conformal factor, (r, θ) is the radial and angular coordinates in 2D spherical coordinates, and $m \geq 1$ is the toroidal magnetization index.

The toroidal magnetic field corresponds to a field aligned with the ϕ -direction in spherical coordinates (see e.g. [80] for a depiction of a toroidal magnetic field). As discussed in Section I, purely toroidal field configurations are generally considered unstable. However, by employing 2D axisymmetry in our simulations, the magnetic instabilities associated with this configuration are suppressed. Nevertheless, many studies in the literature report instability even in mixed-field configurations (see e.g. [26]). As the stable magnetic field configuration remains uncertain, this work provides an initial investigation into the fundamental modes of rotating neutron stars with a purely toroidal magnetic field setup.

All models share the same toroidal magnetization index $m = 1$ but differ in the value of the toroidal magnetization constant, K_m . To investigate the effects of the toroidal magnetic field, we construct equilibrium models in 5 sequences with $K_m \in \{0.5, 1.0, 1.5, 2.0, 2.5\}$, each corresponding to a maximum magnetic field strength of $\mathcal{B}_{\max} \sim \mathcal{O}(10^{17})$ G. As mentioned in Section I, such a field strength has been shown to suppress the fundamental mode frequency of neutron stars in our previous work [59].

Since this work does not aim to investigate neutron stars with varying masses, we adopt a fixed baryonic mass of $M_0 = 1.506$ for all models. Three high-mass neutron stars have been observed recently: J0348+0432 with $M = 2.01 \pm 0.04$ [81], PSR J0740+6620 with $M = 2.08 \pm 0.07$ [82], and PSR J0952-0607 with $M = 2.35 \pm 0.17$ [75]. These observations indicate that the maximum mass of a neutron star should be at least $M = 2.0$. Consequently, the masses of our models fall within the observational constraints on the maximum mass of a neutron star. Additionally, the adopted baryonic mass $M_0 = 1.506$ is identical to that used in previous studies [49, 54], allowing for direct comparison with these works.

By fixing the baryonic mass, we aim to clarify the qualitative trends in how mode frequencies vary with rotation and toroidal magnetic field strength. However, if the mass were not fixed but allowed to vary, both the mode frequencies and quantitative aspects, such as the slopes and intercepts of the linear fits discussed in Sections III and IV, would be expected to change. Therefore, a more comprehensive study that explores a range of baryonic masses, including values close to 2.0, which are especially relevant for binary neutron star merger remnants, will be necessary for a more general determination of mode frequencies. Such an analysis is beyond the scope of this study and will be addressed in future work.

The detailed properties of the equilibrium models used in this study are summarized in Appendix A.

B. Evolutions

We use the new general relativistic magnetohydrodynamics code **Gmunu** [64–66] to evolve the stellar models in dynamical spacetime. The models are evolved over a time of 20 ms using a polytropic equation of state, $P = K\rho^\gamma$, with the same parameters as the equilibrium models (i.e. $K = 100$ and $\gamma = 2$).

We perform 2D ideal general-relativistic magnetohydrodynamics (GRMHD) simulations in axisymmetry about the z -axis, assuming equatorial symmetry and employing spherical coordinates (r, θ) . The computational domain spans $0 \leq r \leq 60$ and $0 \leq \theta \leq \pi/2$, with a base grid resolution of $N_r \times N_\theta = 64 \times 16$. AMR with 4 levels is used, achieving an effective resolution of 512×128 . The AMR refinement criteria follow those described in [59, 65]. Our simulations employ a total variation diminishing Lax-Friedrichs (TVDLF) approximate Riemann solver [83], a third-order reconstruction method using the piecewise parabolic method (PPM) [84] and a third-order accurate strong stability-preserving Runge-Kutta (SSPRK3) time integrator [85]. An artificial atmosphere with a rest-mass density $\rho_{\text{atm}} \sim 10^{-10} \rho_c$ is imposed outside the star. Furthermore, no divergence cleaning method is applied in these simulations since they are restricted to magnetized stars with a purely toroidal magnetic field in axisymmetry.

C. Initial perturbations

By applying the following fluid perturbations in the initial time-slice, we excite the 2 fundamental modes of neutron stars [49].

First, the fundamental $l = 0$ quasi-radial mode (i.e. F -mode) is excited by the $l = 0$ perturbation on the r -component of the three-velocity field v^r ,

$$\delta v^r = a \sin \left[\pi \frac{r}{r_s(\theta)} \right], \quad (4)$$

where $r_s(\theta)$ denotes the radial position of the stellar surface, and the perturbation amplitude a (in the unit of c) is chosen to be -0.005.

Second, the fundamental $l = 2$ quadrupolar mode (i.e. $2f$ -mode) is excited by the $l = 2$ perturbation on the θ -component of the three-velocity field v^θ ,

$$\delta v^\theta = a \sin \left[\pi \frac{r}{r_s(\theta)} \right] \sin \theta \cos \theta, \quad (5)$$

where a is chosen to be 0.01.

We extract the fundamental modes by performing Fourier transforms of v^r and v^θ at $r = 3$ and $\theta = \pi/4$, ensuring that the extraction position lies within the star (see [49] for further details).

III. FUNDAMENTAL MODE FREQUENCIES AGAINST STELLAR COMPACTNESS

Our previous work have shown the quasi-linearity between the fundamental mode frequency and the stellar compactness for rotating neutron stars without a magnetic field [54]. To determine whether the presence of a toroidal magnetic field affects this relation, we plot the fundamental $l = 0$ quasi-radial mode frequency f_F (top left panel) and fundamental $l = 2$ quadrupolar mode frequency f_{2f} (bottom left panel) against the stellar compactness M/R in Fig. 1, where M is the gravitational mass and R is the circumferential radius. The data points are arranged into 5 sequences with $K_m \in \{0.5, 1.0, 1.5, 2.0, 2.5\}$, where K_m is the toroidal magnetization constant quantifying the toroidal magnetic field strength. As a comparison, we also include data from sequence A of Yip et al. [54], which investigates the fundamental modes of unmagnetized neutron stars undergoing uniform rotation. As in the unmagnetized case (sequence A), both f_F and f_{2f} increase approximately linearly with M/R for all values of K_m .

Hence, we perform linear regressions using the data from our simulations and sequence A to quantify f_F and f_{2f} as functions of the stellar compactness M/R for rotating neutron stars with a purely toroidal magnetic field. For the quasi-radial $l = 0$ fundamental mode frequency f_F^{pred} ,

$$f_F^{\text{pred}}(\text{kHz}) \approx a_0^F - a_1^F \frac{M}{R}, \quad (6)$$

where the residues of $f_F^{\text{pred}}(M/R)$ are $\lesssim 1\%$. For the quadrupolar $l = 2$ fundamental mode frequency f_{2f}^{pred} ,

$$f_{2f}^{\text{pred}}(\text{kHz}) \approx a_0^{2f} - a_1^{2f} \frac{M}{R}, \quad (7)$$

where the residues of $f_{2f}^{\text{pred}}(M/R)$ are $\lesssim 1\%$.

To better illustrate how the slopes of the linear fits $f^{\text{pred}}(M/R)$ change with K_m , we plot a_1^F (top right panel) and a_1^{2f} (bottom right panel) against the toroidal magnetization constant K_m in Fig. 1. We observe that the slopes a_1^F and a_1^{2f} deviate from the unmagnetized case. Specifically, a_1^F decreases with increasing K_m , whereas a_1^{2f} increases with K_m . Hence, this demonstrates that the quasi-linear relation between the fundamental mode frequency and stellar compactness remains valid for rotating neutron stars in the presence of a toroidal magnetic field, although the field strength, quantified by K_m , modifies the slope of the relation.

IV. FUNDAMENTAL MODE FREQUENCIES AGAINST KINETIC-TO-BINDING ENERGY RATIO

As mentioned in Section I, our previous work has updated the linear relations for quantifying fundamental

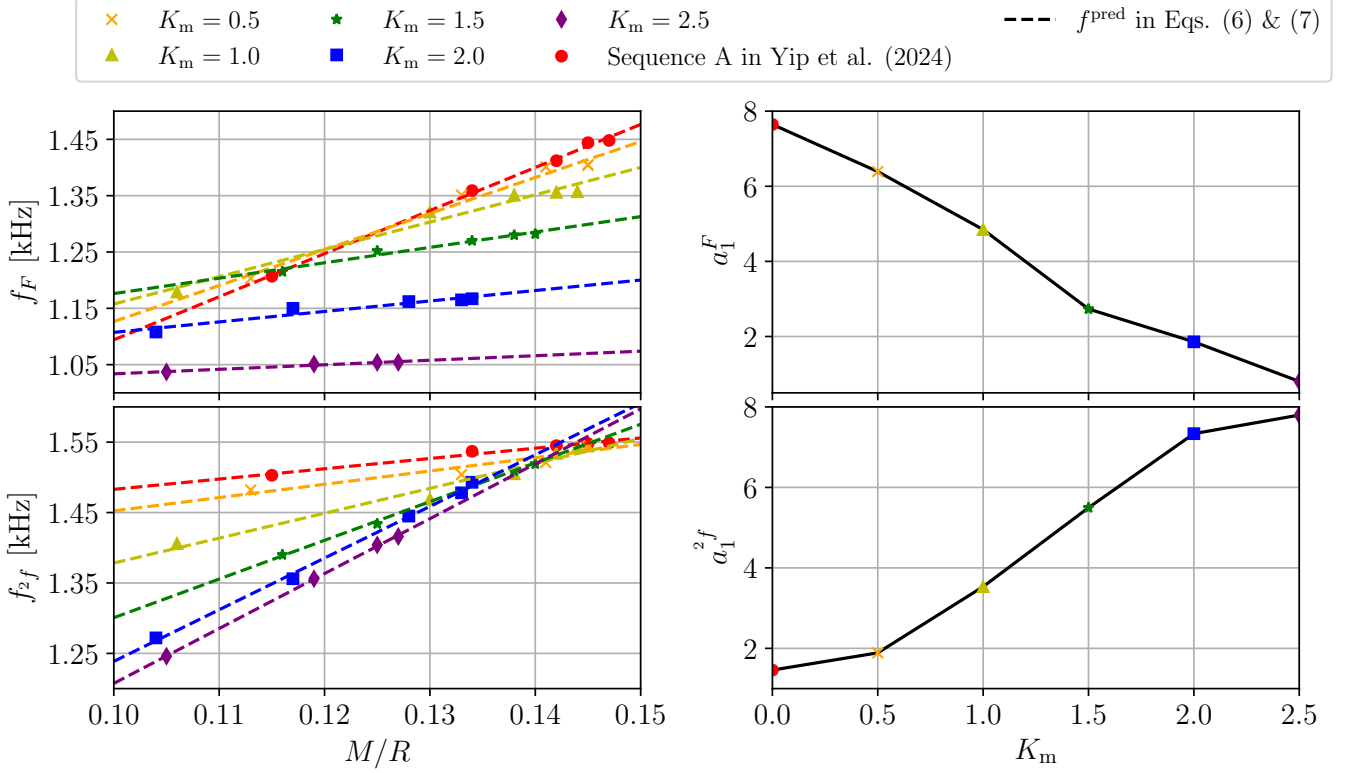


FIG. 1: Plots of fundamental mode frequencies f against the stellar compactness M/R (left panels), where M is the gravitational mass and R is the circumferential radius, and the corresponding slopes a_1 of the linear fits $f^{\text{pred}}(M/R)$ against the toroidal magnetization constant K_m (right panels). Specifically, we plot the fundamental $l = 0$ quasi-radial mode frequency f_F (top left panel) and the fundamental $l = 2$ quadrupolar mode frequency f_{2f} (bottom left panel) against M/R . The corresponding slopes of the linear fits a_1^F (top right panel) and a_1^{2f} (bottom right panel) are plotted against K_m . Data points represent five sequences with $K_m \in \{0.5, 1.0, 1.5, 2.0, 2.5\}$, where K_m quantifies the strength of the toroidal magnetic field. For comparison, we also include data from sequence A of Yip et al. [54], which investigates the fundamental modes of unmagnetized neutron stars undergoing uniform rotation. As in the unmagnetized case (sequence A), both f_F and f_{2f} increase approximately linearly with M/R for all values of K_m . Linear regressions are performed to obtain the predicted linear fit $f^{\text{pred}}(M/R)$ in the form of Eqs. (6) and (7) for each sequence (dashed lines). We observe that the slopes a_1^F and a_1^{2f} deviate from the unmagnetized case: a_1^F decreases with K_m while a_1^{2f} increases with K_m . Therefore, this demonstrates that the quasi-linear relation between the fundamental mode frequency and stellar compactness remains valid for rotating neutron stars in the presence of a toroidal magnetic field, although the field strength, quantified by K_m , modifies the slope of the relation.

$l = 0$ quasi-radial mode frequency f_F and fundamental $l = 2$ quadrupolar mode frequency f_{2f} of rotating neutron stars based on the kinetic-to-binding energy ratio $T/|W|$ by considering both the effect of dynamical spacetime and various degrees of differential rotation for the first time [54]. Nevertheless, a magnetic field is not taken into account in constructing the relations. Hence, we revisit the relation between the fundamental mode frequency f and kinetic-to-binding energy ratio $T/|W|$ by considering the presence of a toroidal magnetic field. In Fig 2, we plot the frequency of the fundamental $l = 0$ quasi-radial mode f_F (top left panel) and the fundamental $l = 2$ quadrupolar mode f_{2f} (bottom left panel) against the kinetic-to-binding energy ratio

$T/|W|$. The data points are grouped into five sequences with $K_m \in \{0.5, 1.0, 1.5, 2.0, 2.5\}$. For all K_m values, f_F increases approximately linearly with $T/|W|$.

Thus, we perform linear regressions using our simulation data to obtain a linear fit for each sequence to quantify the fundamental $l = 0$ quasi-radial mode frequency f_F and fundamental $l = 2$ quadrupolar mode frequency f_{2f} as functions of the kinetic-to-binding energy ratio $T/|W|$ for rotating neutron stars with a purely toroidal magnetic field. For the quasi-radial $l = 0$ fundamental mode frequency f_F^{pred} ,

$$f_F^{\text{pred}}(\text{kHz}) \approx b_0^F - b_1^F \frac{T}{|W|}, \quad (8)$$

where the residues of $f_F^{\text{pred}}(T/|W|)$ are $\lesssim 2\%$. For the quadrupolar $l = 2$ fundamental mode frequency f_{2f}^{pred} ,

$$f_{2f}^{\text{pred}}(\text{kHz}) \approx b_0^{2f} - b_1^{2f} \frac{T}{|W|}, \quad (9)$$

where the residues of $f_{2f}^{\text{pred}}(T/|W|)$ are $\lesssim 1\%$. We also include the relations proposed in Eqs. (4) and (5) of our previous work [54] (red solid line). For the quasi-radial $l = 0$ fundamental mode frequency f_F^{pred} ,

$$f_F^{\text{pred}}(\text{kHz}) \approx 1.45 - 3.42 \frac{T}{|W|}. \quad (10)$$

For the quadrupolar $l = 2$ fundamental mode frequency f_{2f}^{pred} ,

$$f_{2f}^{\text{pred}}(\text{kHz}) \approx 1.56 - 0.65 \frac{T}{|W|}. \quad (11)$$

To better illustrate how the slopes of the linear fits $f^{\text{pred}}(T/|W|)$ change with K_m , we plot b_1^F (top right panel) and b_1^{2f} (bottom right panel) against the toroidal magnetization constant K_m in Fig. 2. We observe that the slopes b_1^F and b_1^{2f} deviate from the unmagnetized case (Yip et al.). In particular, b_1^F increases with K_m while b_1^{2f} decreases with K_m . Accordingly, the quasi-linear relation between the fundamental mode frequency and the kinetic-to-binding energy ratio still holds for rotating neutron stars when a toroidal magnetic field is present, though the field strength, quantified by K_m , modifies the slope of the relation.

V. CONSTRAINING THE MAGNETIC FIELD AND THE ROTATION

To better illustrate the correlation between the fundamental mode frequencies and the properties of the rotating magnetized neutron star, we plot a contour plot of the frequency ratio between the fundamental $l = 0$ quasi-radial mode and the fundamental $l = 2$ quadrupolar mode f_{2f}/f_F against the kinetic-to-binding energy ratio $T/|W|$ (horizontal axis) and the maximum magnetic field strength \mathcal{B}_{max} (vertical axis) in Fig. 3. We constructed this plot by the multiquadric radial basis function interpolation of the data points of our models and the models in Sequence A of Yip et al. [54]. A colored dot with a black edge labels each data point. The dash-dotted lines denote the contour lines for particular values of f_{2f}/f_F . We use $T/|W|$ to quantify rotation instead of the rotational angular velocity Ω because $T/|W|$ can be generalized to cases with differential rotation, where no unique value of Ω is sufficient to describe the rotation. The effects of differential rotation are further discussed in Section VI. For a fixed value of f_{2f}/f_F , there are localized regions in the $T/|W|$ - \mathcal{B}_{max} plane. Therefore, the measurement of f_{2f}/f_F constrains the values of $T/|W|$ and \mathcal{B}_{max} .

VI. IMPACT OF DIFFERENTIAL ROTATION

As discussed in Section I, neutron stars could exhibit differential rotation in some astrophysical scenarios, such as core-collapse supernovae and binary neutron star mergers (see e.g. [3–5] for reviews). In this section, we investigate the deviations caused by differential rotation in comparison to the fundamental mode frequency predicted by the linear relations $f^{\text{pred}}(T/|W|)$ obtained for uniformly rotating cases in Section IV.

A variety of differential rotation laws have been proposed in the literature to describe the differential rotation of protoneutron stars and binary neutron star merger remnants (see e.g. [40, 86–88]). However, since the primary focus of this section is on the effects of the degree of differential rotation rather than the detailed differences among rotation laws, we adopt a simplified case of the j -constant differential rotation law [89, 90], which models differential rotation in neutron stars as,

$$j(\Omega) = A^2 (\Omega_c - \Omega), \quad (12)$$

where j is the relativistic specific angular momentum, A is a parameter controlling the degree of differential rotation, Ω is the angular velocity, and Ω_c is the central angular velocity.

The j -constant law is widely used to model differentially rotating neutron stars (e.g. [91–93]). Following previous studies (e.g. [50, 54]), we adopt the parameter $\tilde{A} = (A/r_e)^{-1}$ to quantify the degree of differential rotation, where r_e is the equatorial radius of the equilibrium model. As we do not intend to conduct a comprehensive survey of the effects of \tilde{A} and K_m , we fix $\tilde{A} = 1$ and select two representative, extreme values of $K_m \in 0.5, 2.5$ for this study. The adopted values of K_m correspond to the lowest and highest toroidal magnetization constants considered, thereby allowing us to estimate the impact of differential rotation across the range of magnetic field strengths relevant to our models. The choice of $\tilde{A} = 1$ is motivated by its widespread use in studies of oscillations in differentially rotating neutron stars (see e.g. [32, 49]) and it is physically representative because it yields a degree of differential rotation similar to that typically observed in core-collapse supernova simulations (see e.g. [94]). Therefore, our parameter choices are representative of physically relevant scenarios and enable us to capture the essential effects of differential rotation and magnetic fields within a manageable computational framework.

In Fig. 4, we plot fundamental mode frequencies f (top panels) and the frequency deviations between the simulation data f^{data} of differentially rotating (DR) neutron star and the predictions by linear fits constructed with the data of uniformly rotating (UR) neutron star $f_{\text{UR}}^{\text{pred}}$ (bottom panels) against kinetic-to-binding energy ratio $T/|W|$. In particular, we plot fundamental $l = 0$ quasi-radial mode frequency f_F (top left panel), deviation of

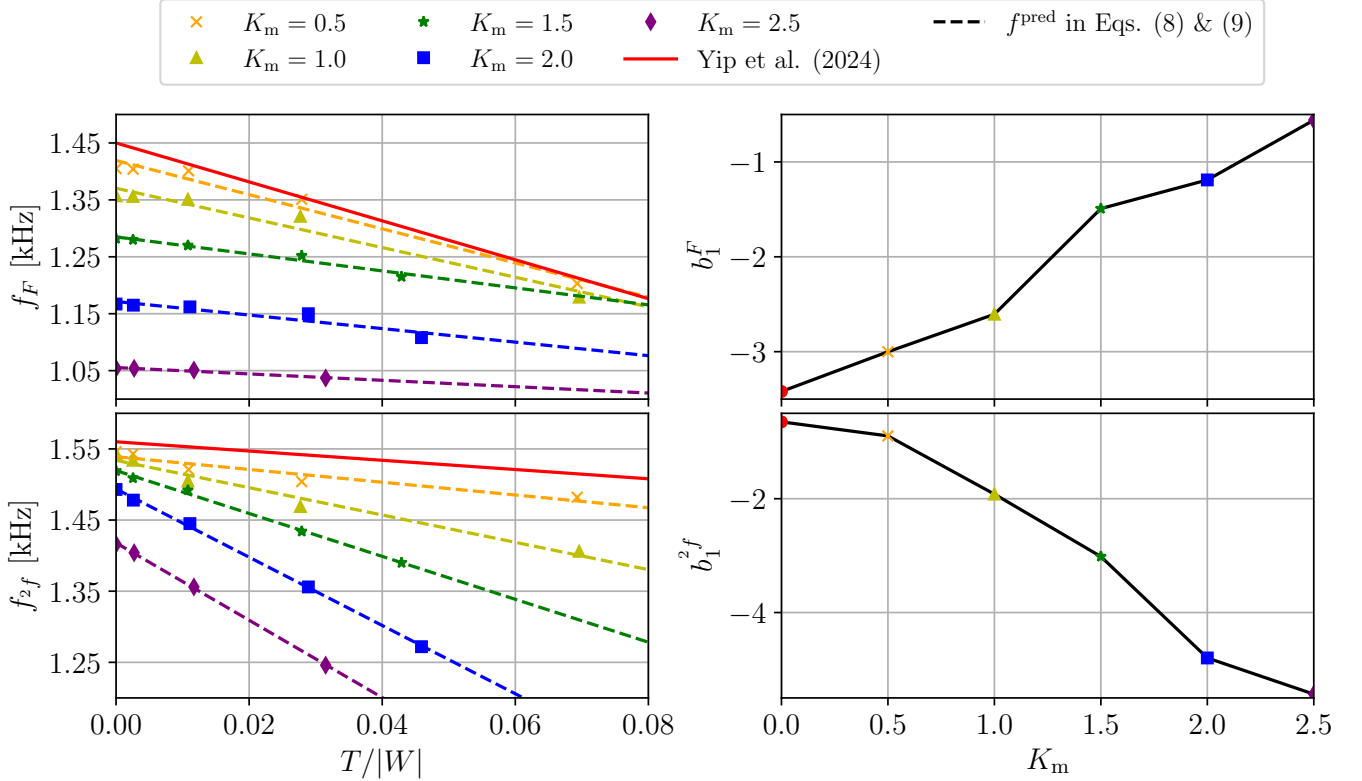


FIG. 2: Plots of fundamental mode frequencies f against the kinetic-to-binding energy ratio $T/|W|$ (left panels) and the corresponding slopes b_1 of the linear fits $f^{\text{pred}}(T/|W|)$ against the toroidal magnetization constant K_m (right panels). Specifically, we plot the fundamental $l = 0$ quasi-radial mode frequency f_F (top left panel) and the fundamental $l = 2$ quadrupolar mode frequency f_{2f} (bottom left panel) against $T/|W|$. The corresponding slopes of the linear fits b_1^F (top right panel) and b_1^{2f} (bottom right panel) are plotted against K_m . The data points are grouped into five sequences with $K_m \in \{0.5, 1.0, 1.5, 2.0, 2.5\}$, where K_m quantifies the toroidal field strength. Both f_F and f_{2f} increase approximately linearly with $T/|W|$ for all K_m . Accordingly, linear regressions are performed to obtain the predicted linear fit $f^{\text{pred}}(T/|W|)$ in the form of Eqs. (8) and (9) for each sequence (dashed lines). We also compare with the predictions f_F^{pred} and f_{2f}^{pred} in Eqs. (4) and (5) of our previous work of Yip et al. [54] (red solid lines). This prediction was based on the fundamental modes of rotating neutron stars with differential rotation but without magnetic fields. We observe that the slopes b_1^F and b_1^{2f} deviate from the unmagnetized case (Yip et al.): b_1^F increases with K_m while b_1^{2f} decreases with K_m . Therefore, the quasi-linear relation between the fundamental mode frequency and the kinetic-to-binding energy ratio still holds for rotating neutron stars when a toroidal magnetic field is present, though the field strength, quantified by K_m , modifies the slope of the relation.

f_F (bottom left panel), fundamental $l = 2$ quadrupolar mode frequency f_{2f} (top right panel), and deviation of f_{2f} (bottom right panel) against $T/|W|$. The data points are grouped into 2 sequences of DR neutron star with $K_m \in \{0.5, 2.5\}$. We find that only a slight deviation between f^{data} and $f_{\text{UR}}^{\text{pred}}$ with $f_F^{\text{data}}/f_F^{\text{pred}} - 1 \lesssim 2.5\%$ and $f_{2f}^{\text{data}}/f_{2f}^{\text{pred}} - 1 \lesssim 5\%$. Consequently, differential rotation in the examined models introduces only minor deviations in the fundamental mode frequencies compared to the predictions from linear relations derived for uniformly rotating cases.

Adopting a simplified j -constant differential rotation law with a fixed value of $\tilde{A} = 1$ and representative val-

ues of K_m is expected to capture the qualitative trend of the quasi-linear behavior observed in the mode frequencies of magnetized neutron stars with differential rotation. However, this assumption may result in quantitative differences in the computed mode frequencies and, consequently, in deviations from the predicted linear fits, particularly for configurations outside the explored parameter space or those with more realistic rotation laws. Therefore, a more comprehensive exploration of the parameter space of \tilde{A} and K_m , together with the adoption of more realistic rotation laws, is necessary to determine the precise range of validity of these findings.

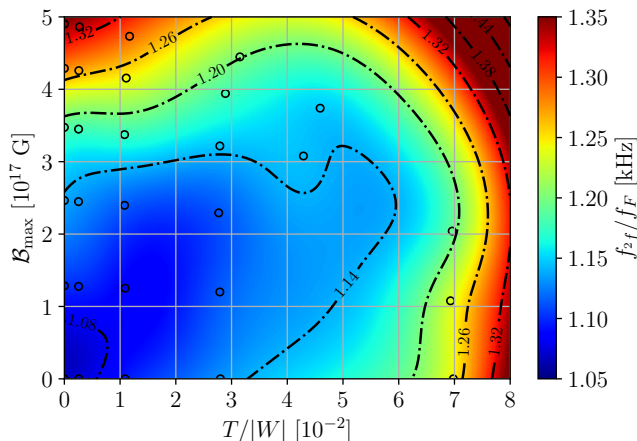


FIG. 3: Contour plot of the frequency ratio between the fundamental $l = 0$ quasi-radial mode and the fundamental $l = 2$ quadrupolar mode f_{2f}/f_F against the kinetic-to-binding energy ratio $T/|W|$ (horizontal axis) and the maximum magnetic field strength B_{\max} (vertical axis). This plot is constructed by the multiquadric radial basis function interpolation of the data points of our models and the models in Sequence A of Yip et al. [54]. Each data point is labeled by a colored dot with a black edge. The dash-dotted lines denote the contour lines for particular values of f_{2f}/f_F . Values of f_{2f}/f_F are located in specific regions of the $B_{\max} - T/|W|$ plane. In consequence, measuring f_{2f}/f_F allows one to infer the value of B_{\max} and $T/|W|$.

VII. CONCLUSIONS

In this work, for the first time, we considered a magnetic field to construct linear relations quantifying the frequencies of fundamental $l = 0$ quasi-radial mode f_F and fundamental $l = 2$ quadrupolar mode f_{2f} . In particular, through linear regression of our simulated data, we found that the quasi-linearity between fundamental mode frequency f , stellar compactness M/R , the ratio of kinetic energy to binding energy $T/|W|$ remains valid but the slope is controlled by the toroidal magnetization constant K_m quantifying the toroidal magnetic field strength. Next, we demonstrated that measuring the frequency ratio between the two fundamental modes f_{2f}/f_F can infer the kinetic-to-binding energy ratio $T/|W|$ and the maximum magnetic field strength B_{\max} . Furthermore, we examined 2 sequences of differentially rotating neutron star models with $K_m \in \{0.5, 2.5\}$ and show that differential rotations only introduces minor deviations in the fundamental mode frequencies compared to the predictions from linear relations derived for uniformly rotating cases in the examined models.

The fundamental modes discussed in this study lie in the frequency range of $f \sim 1200 - 1600$ Hz. Current gravitational wave detectors, such as Advanced LIGO [95], Advanced Virgo [96], and KAGRA [97, 98], are sen-

sitive to gravitational wave signals within a frequency range of $f \sim 20 - 2000$ Hz. Consequently, these detectors can only barely detect the modes in this range. On the other hand, third-generation gravitational wave detectors, including the Einstein Telescope (ET) [99] and Cosmic Explorer (CE) [100–102], are designed for a significantly broader sensitivity band, covering frequencies from $f \sim 1 - 10000$ Hz. Moreover, it has been shown that the dominant mode frequency of the post-merger signal from binary neutron star coalescences at a distance of 68 Mpc can be measured with an accuracy of $\sim \mathcal{O}(10)$ Hz for post-merger signals with a signal-to-noise ratio of ~ 10 using third-generation detectors [103]. Assuming that the fundamental modes studied here can be measured with similar accuracy, and considering that the mode frequencies lie within the range $f \sim 1200 - 1600$ Hz while the frequency ratio spans $f_{2f}/f_F \sim 1.05 - 1.35$ (as shown in Fig. 3), we expect that the frequency ratio f_{2f}/f_F can be determined with an error of $\lesssim 1\%$. This measurement uncertainty would translate to an error bar of comparable width ($\lesssim 1\%$) when inferring the kinetic-to-binding energy ratio $T/|W|$ and the maximum magnetic field strength B_{\max} with the contour plot in Fig. 3. However, a thorough analysis focused on gravitational waves emitted by rotating neutron stars is required to confirm this claim. Such an investigation falls outside the scope of the present study and is left for future work.

Several extensions to the current work could be made. Firstly, a broader investigation covering a wide range of baryonic masses, including those approaching 2.0 , which are particularly relevant for merger remnants of binary neutron stars, would be beneficial to more generally characterize mode frequencies. Additionally, for a more precise determination of oscillation modes in neutron stars, especially in contexts such as core-collapse supernovae and neutron star mergers, it is crucial to implement more realistic equations of state that account for thermal effects (see e.g. [5, 104]) and to consider empirically motivated rotation profiles (see e.g. [40, 71, 72, 86–88]), as have been proposed for modeling such scenarios. Moreover, it would be worthwhile to explore alternative magnetic field configurations, including purely poloidal fields and twisted torus structures. Finally, since the present work restricts itself to axisymmetry, thereby suppressing the instability associated with purely toroidal fields, future studies should include fully 3D simulations without this symmetry constraint. This would allow investigation of the stability and the emergence of non-axisymmetric oscillation modes, which could play a crucial role in the dynamics of binary neutron star remnants and proto-neutron stars formed in core-collapse supernovae (see e.g. [67]).

ACKNOWLEDGMENTS

We acknowledge the support of the CUHK Central High-Performance Computing Cluster, on which the sim-

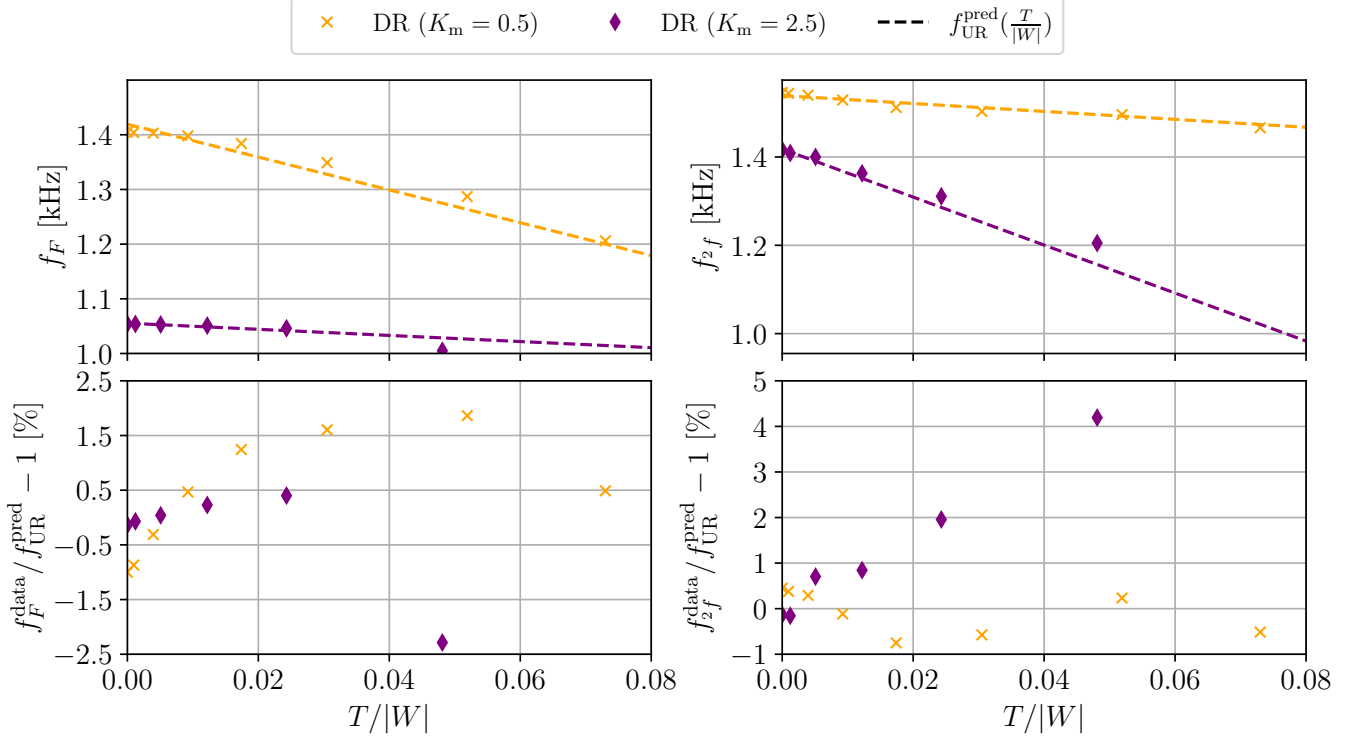


FIG. 4: Plots of fundamental mode frequencies f (top panels) and the frequency deviations between the simulation data f^{data} of differentially rotating (DR) neutron star and the predictions by linear fits constructed with the data of uniformly rotating (UR) neutron star f_{UR}^{pred} (bottom panels) against kinetic-to-binding energy ratio $T/|W|$. In particular, we plot fundamental $l=0$ quasi-radial mode frequency f_F (top left panel), deviation of f_F (bottom left panel), fundamental $l=2$ quadrupolar mode frequency f_{2f} (top right panel), and deviation of f_{2f} (bottom right panel) against $T/|W|$. The data points are grouped into 2 sequences of DR neutron star with $K_m \in \{0.5, 2.5\}$. We find that only a slight deviation between f^{data} and f_{UR}^{pred} with $f_F^{\text{data}}/f_F^{\text{pred}} - 1 \lesssim 2.5\%$ and $f_{2f}^{\text{data}}/f_{2f}^{\text{pred}} - 1 \lesssim 5\%$. Thus, we found that differential rotation in the examined models introduces only minor deviations in the fundamental mode frequencies compared to the predictions from linear relations derived for uniformly rotating cases.

ulations in this work have been performed. This work was partially supported by grants from the Research Grants Council of Hong Kong (Project No. CUHK 14306419), the Croucher Innovation Award from the Croucher Foundation Hong Kong, and the Direct Grant for Research from the Research Committee of The Chinese University of Hong Kong.

Appendix A: Equilibrium models of neutron stars

This appendix summarizes the detailed properties of the equilibrium models used in this study. Tables A1 – A5 present the stellar properties of the equilibrium models for the sequences TK1U, TK2U, TK3U, TK4U, and TK5U. These sequences represent uniformly rotating neutron stars with a fixed rest mass of $M_0 = 1.506$ and toroidal magnetization constants $K_m \in \{0.5, 1.0, 1.5, 2.0, 2.5\}$, respectively. The data in these tables were discussed and used to construct the linear fits described in Sections III and IV of the main

text. Tables A6– A7 summarize the properties of the equilibrium models for the sequences TK1D and TK5D. These sequences represent differentially rotating neutron stars modeled by the j -constant law with $\tilde{A} = 1.0$, a fixed rest mass of $M_0 = 1.506$, and toroidal magnetization constants $K_m \in \{0.5, 2.5\}$, respectively. The data are provided in the form of one table for each sequence. Each table lists the model, the central rest mass density ρ_c , the gravitational mass M , the circumferential radius R , the maximum magnetic field strength \mathcal{B}_{max} , the central angular velocity Ω_c , and the ratio of rotational kinetic energy T to the absolute value of gravitational binding energy $T/|W|$.

Model	ρ_c (10^{-3})	M	R	\mathcal{B}_{\max} (10^{17} G)	Ω_c (10^{-2})	$T/ W $
TK1U0	1.290	1.401	9.638	1.285	0.000	0.000
TK1U1	1.275	1.402	9.687	1.277	0.500	0.003
TK1U2	1.225	1.403	9.972	1.252	1.000	0.011
TK1U3	1.130	1.407	10.544	1.200	1.500	0.028
TK1U4	0.924	1.415	12.484	1.078	2.000	0.069

TABLE A1: Stellar properties of the equilibrium models of sequence TK1U constructed by the XNS code. TK1U is a sequence of uniformly rotating neutron star with a fixed rest mass $M_0 = 1.506$ and toroidal magnetization constant $K_m = 0.5$. ρ_c is the central density, M is the gravitational mass, R is the circumferential radius, \mathcal{B}_{\max} is the maximum magnetic field strength, Ω_c is the central angular velocity, $T/|W|$ is the ratio of rotational kinetic energy T to the absolute value of gravitational binding energy $|W|$. Numerical values of these stellar properties are rounded off to three decimal places.

Model	ρ_c (10^{-3})	M	R	\mathcal{B}_{\max} (10^{17} G)	Ω_c (10^{-2})	$T/ W $
TK2U0	1.316	1.404	9.773	2.464	0.000	0.000
TK2U1	1.301	1.404	9.868	2.448	0.500	0.003
TK2U2	1.253	1.406	10.154	2.397	1.000	0.011
TK2U3	1.159	1.409	10.819	2.293	1.500	0.028
TK2U4	0.954	1.418	13.319	2.041	2.000	0.070

TABLE A2: Stellar properties of the equilibrium models of sequence TK2U constructed by the XNS code. TK2U is a sequence of uniformly rotating neutron star with a fixed rest mass $M_0 = 1.506$ and toroidal magnetization constant $K_m = 1.0$.

Model	ρ_c (10^{-3})	M	R	\mathcal{B}_{\max} (10^{17} G)	Ω_c (10^{-2})	$T/ W $
TK3U0	1.344	1.408	10.094	3.474	0.000	0.000
TK3U1	1.329	1.409	10.189	3.450	0.500	0.003
TK3U2	1.282	1.411	10.521	3.374	1.000	0.011
TK3U3	1.189	1.414	11.280	3.217	1.500	0.028
TK3U4	1.112	1.417	12.177	3.079	1.750	0.043

TABLE A3: Stellar properties of the equilibrium models of sequence TK3U constructed by the XNS code. TK3U is a sequence of uniformly rotating neutron star with a fixed rest mass $M_0 = 1.506$ and toroidal magnetization constant $K_m = 1.5$.

Model	ρ_c (10^{-3})	M	R	\mathcal{B}_{\max} (10^{17} G)	Ω_c (10^{-2})	$T/ W $
TK4U0	1.362	1.414	10.554	4.289	0.000	0.000
TK4U1	1.347	1.414	10.650	4.258	0.500	0.003
TK4U2	1.299	1.416	11.076	4.155	1.000	0.011
TK4U3	1.204	1.419	12.117	3.942	1.500	0.029
TK4U4	1.119	1.423	13.718	3.739	1.750	0.046

TABLE A4: Stellar properties of the equilibrium models of sequence TK4U constructed by the XNS code. TK4U is a sequence of uniformly rotating neutron star with a fixed rest mass $M_0 = 1.506$ and toroidal magnetization constant $K_m = 2.0$.

Model	ρ_c (10^{-3})	M	R	\mathcal{B}_{\max} (10^{17} G)	Ω_c (10^{-2})	$T/ W $
TK5U0	1.362	1.420	11.203	4.902	0.000	0.000
TK5U1	1.347	1.421	11.345	4.862	0.500	0.003
TK5U2	1.297	1.422	11.913	4.732	1.000	0.012
TK5U3	1.194	1.426	13.612	4.448	1.500	0.032

TABLE A5: Stellar properties of the equilibrium models of sequence TK5U constructed by the XNS code. TK5U is a sequence of uniformly rotating neutron star with a fixed rest mass $M_0 = 1.506$ and toroidal magnetization constant $K_m = 2.5$.

Model	ρ_c (10^{-3})	M	R	\mathcal{B}_{\max} (10^{17} G)	Ω_c (10^{-2})	$T/ W $
TK1D0	1.290	1.401	9.638	1.285	0.000	0.000
TK1D1	1.284	1.401	9.639	1.283	0.500	0.001
TK1D2	1.264	1.402	9.734	1.275	1.000	0.004
TK1D3	1.229	1.403	9.831	1.260	1.500	0.009
TK1D4	1.176	1.404	10.023	1.239	2.000	0.017
TK1D5	1.096	1.407	10.405	1.204	2.500	0.031
TK1D6	0.974	1.411	10.979	1.148	3.000	0.052
TK1D7	0.864	1.416	11.646	1.094	3.500	0.073

TABLE A6: Stellar properties of the equilibrium models of sequence TK1D constructed by the XNS code. TK1D is a sequence of differentially rotating neutron star with a fixed rest mass $M_0 = 1.506$ and toroidal magnetization constant $K_m = 0.5$.

Model	ρ_c (10^{-3})	M	R	\mathcal{B}_{\max} (10^{17} G)	Ω_c (10^{-2})	$T/ W $
TK5D0	1.362	1.420	11.203	4.902	0.000	0.000
TK5D1	1.354	1.421	11.250	4.885	0.500	0.001
TK5D2	1.332	1.421	11.393	4.832	1.000	0.005
TK5D3	1.292	1.423	11.725	4.735	1.500	0.012
TK5D4	1.225	1.425	12.246	4.568	2.000	0.024
TK5D5	1.103	1.429	13.617	4.240	2.500	0.048

TABLE A7: Stellar properties of the equilibrium models of sequence TK5D constructed by the XNS code. TK5D is a sequence of differentially rotating neutron star ($\dot{A} = 1.0$) with a fixed rest mass $M_0 = 1.506$ and toroidal magnetization constant $K_m = 2.5$.

-
- [1] A. Reisenegger, Magnetic Fields of Neutron Stars: an Overview, in *Magnetic Fields Across the Hertzsprung-Russell Diagram*, Astronomical Society of the Pacific Conference Series, Vol. 248, edited by G. Mathys, S. K. Solanki, and D. T. Wickramasinghe (2001) p. 469, arXiv:astro-ph/0103010 [astro-ph].
- [2] B. P. Abbott, R. Abbott, T. D. Abbott, S. Abraham, F. Acernese, K. Ackley, C. Adams, R. X. Adhikari, V. B. Adya, C. Affeldt, M. Agathos, K. Agatsuma, N. Aggarwal, O. D. Aguiar, L. Aiello, A. Ain, P. Ajith, G. Allen, A. Allocca, M. A. Aloy, P. A. Altin, A. Amato, S. Anand, A. Ananyeva, S. B. Anderson, W. G. Anderson, S. V. Angelova, S. Antier, S. Appert, K. Arai, M. C. Araya, J. S. Areeda, M. Arène, N. Arnaud, S. M. Aronson, K. G. Arun, S. Ascenzi, G. Ashton, S. M. Aston, P. Astone, F. Aubin, P. Aufmuth, K. AultONeal, C. Austin, V. Avendano, A. Avila-Alvarez, S. Babak, P. Bacon, F. Badaracco, M. K. M. Bader, S. Bae, J. Baird, P. T. Baker, F. Baldaccini, G. Ballardín, S. W. Ballmer, A. Bals, S. Banagiri, J. C. Barayoga, C. Barbieri, S. E. Barclay, B. C. Barish, D. Barker, K. Barkett, S. Barnum, F. Barone, B. Barr, L. Barsotti, M. Barsuglia, D. Barta, J. Bartlett, I. Bartos, R. Bassiri, A. Basti, M. Bawaj, J. C. Bayley, A. C. Baylor, M. Bazzan, B. Bécsy, M. Bejger, I. Belahcene, A. S. Bell, D. Benawal, M. G. Benjamin, B. K. Berger, G. Bergmann, S. Bernuzzi, C. P. L. Berry, D. Bersanetti, A. Bertolini, J. Betzwieser, R. Bhandare, J. Bidler, E. Biggs, I. A. Bilenko, S. A. Bilgili, G. Billingsley, R. Birney, O. Birnholtz, S. Biscans, M. Bisch, S. Biscoveanu, A. Bisht, M. Bitossi, M. A. Bizouard, J. K. Blackburn, J. Blackman, C. D. Blair, D. G. Blair, R. M. Blair, S. Bloemen, F. Bobba, N. Bode, M. Boer, Y. Boetzel, G. Bogert, F. Bondu, R. Bonnand, P. Booker, B. A. Boom, R. Bork, V. Boschi, S. Bose, V. Bossilkov, J. Bosveld, Y. Bouffanais, A. Bozzi, C. Bradaschia, P. R. Brady, A. Bramley, M. Branchesi, J. E. Brau, M. Breschi, T. Briant, J. H. Briggs, F. Brighenti, A. Brillet, M. Brinkmann, P. Brockill, A. F. Brooks, J. Brooks, D. D. Brown, S. Brunett, A. Buikema, T. Bulik, H. J. Bulten, A. Buonanno, D. Buskulic, C. Buy, R. L. Byer, M. Cabero, L. Cadonati, G. Cagnoli, C. Cahillane, J. Calderón Bustillo, T. A. Callister, E. Calloni, J. B. Camp, W. A. Campbell, M. Canepa, K. C. Cannon, H. Cao, J. Cao, G. Carapella, F. Carbognani, S. Caride, M. F. Carney, G. Carullo, J. Casanueva Diaz, C. Casentini, S. Caudill, M. Cavaglià, F. Cavalier, R. Cavalieri, G. Cella, P. Cerdá-Durán, E. Cesarini, O. Chaibi, K. Chakravarti, S. J. Chamberlin, M. Chan, S. Chao, P. Charlton, E. A. Chase, E. Chassande-Mottin, D. Chatterjee, M. Chaturvedi, K. Chatziioannou, B. D. Cheeseboro, H. Y. Chen, X. Chen, Y. Chen, H. P. Cheng, C. K. Cheong, H. Y. Chia, F. Chiadini, A. Chincarini, A. Chiummo, G. Cho, and H. S. Cho, GW190425: Observation of a Compact Binary Coalescence with Total Mass $\sim 3.4 M_{\odot}$, *ApJ* **892**, L3 (2020), arXiv:2001.01761 [astro-ph.HE].
- [3] H. T. Janka, K. Langanke, A. Marek, G. Martínez-Pinedo, and B. Müller, Theory of core-collapse supernovae, *Phys. Rep.* **442**, 38 (2007), arXiv:astro-ph/0612072 [astro-ph].
- [4] M. Shibata, *Numerical Relativity* (World Scientific, 2016).
- [5] L. Baiotti and L. Rezzolla, Binary neutron star mergers: a review of Einstein's richest laboratory, *Reports on Progress in Physics* **80**, 096901 (2017), arXiv:1607.03540 [gr-qc].
- [6] C. Kouveliotou, S. Dieters, T. Strohmayer, J. van Paradijs, G. J. Fishman, C. A. Meegan, K. Hurley, J. Kommers, I. Smith, D. Frail, and T. Murakami, An X-ray pulsar with a superstrong magnetic field in the soft γ -ray repeater SGR1806 - 20, *Nature* **393**, 235 (1998).
- [7] K. Hurley, P. Li, C. Kouveliotou, T. Murakami, M. Ando, T. Strohmayer, J. van Paradijs, F. Vrba, C. Luginbuhl, A. Yoshida, and I. Smith, ASCA Discovery of an X-Ray Pulsar in the Error Box of SGR 1900+14, *ApJ* **510**, L111 (1999), arXiv:astro-ph/9811388 [astro-ph].
- [8] S. Mereghetti and L. Stella, The Very Low Mass X-Ray Binary Pulsars: A New Class of Sources?, *ApJ* **442**, L17 (1995).
- [9] S. Mereghetti, D. Cremonesi, M. Feroci, and M. Tavani, BeppoSAX observations of SGR 1806-20 SAX observations of SGR 1806-20, *A&A* **361**, 240 (2000).
- [10] J. van Paradijs, R. E. Taam, and E. P. J. van den Heuvel, On the nature of the 'anomalous' 6-s X-ray pulsars, *A&A* **299**, L41 (1995).
- [11] K. Kiuchi and S. Yoshida, Relativistic stars with purely toroidal magnetic fields, *Phys. Rev. D* **78**, 044045 (2008), arXiv:0802.2983 [astro-ph].
- [12] K. Kiuchi, K. Kotake, and S. Yoshida, Equilibrium Configurations of Relativistic Stars with Purely Toroidal Magnetic Fields: Effects of Realistic Equations of State, *ApJ* **698**, 541 (2009), arXiv:0904.2044 [astro-ph.HE].
- [13] J. Friebe and L. Rezzolla, Equilibrium models of relativistic stars with a toroidal magnetic field, *MNRAS* **427**, 3406 (2012), arXiv:1207.4035 [gr-qc].
- [14] M. Bocquet, S. Bonazzola, E. Gourgoulhon, and J. Novak, Rotating neutron star models with a magnetic field., *A&A* **301**, 757 (1995), arXiv:gr-qc/9503044 [gr-qc].
- [15] K. Konno, Moments of inertia of relativistic magnetized stars, *A&A* **372**, 594 (2001), arXiv:gr-qc/0105015 [gr-qc].
- [16] S. S. Yazadjiev, Relativistic models of magnetars: Non-perturbative analytical approach, *Phys. Rev. D* **85**, 044030 (2012), arXiv:1111.3536 [gr-qc].
- [17] S. Bonazzola and E. Gourgoulhon, Gravitational waves from pulsars: emission by the magnetic-field-induced distortion., *A&A* **312**, 675 (1996), arXiv:astro-ph/9602107 [astro-ph].
- [18] R. J. Tayler, Hydromagnetic Instabilities of an Ideally Conducting Fluid, *Proceedings of the Physical Society B* **70**, 31 (1957).
- [19] R. J. Tayler, The adiabatic stability of stars containing magnetic fields-I. Toroidal fields, *MNRAS* **161**, 365 (1973).
- [20] P. Markey and R. J. Tayler, The adiabatic stability of stars containing magnetic fields. II. Poloidal fields, *MNRAS* **163**, 77 (1973).
- [21] P. Markey and R. J. Tayler, The adiabatic stability of stars containing magnetic fields-III. Additional results

- for poloidal fields, *MNRAS* **168**, 505 (1974).
- [22] G. A. E. Wright, Pinch instabilities in magnetic stars, *MNRAS* **162**, 339 (1973).
 - [23] J. Braithwaite and Å. Nordlund, Stable magnetic fields in stellar interiors, *A&A* **450**, 1077 (2006), arXiv:astro-ph/0510316 [astro-ph].
 - [24] J. Braithwaite and H. C. Spruit, Evolution of the magnetic field in magnetars, *A&A* **450**, 1097 (2006), arXiv:astro-ph/0510287 [astro-ph].
 - [25] J. Braithwaite, Axisymmetric magnetic fields in stars: relative strengths of poloidal and toroidal components, *MNRAS* **397**, 763 (2009), arXiv:0810.1049 [astro-ph].
 - [26] A. G. Suvorov and K. Glampedakis, Magnetic equilibria of relativistic axisymmetric stars: The impact of flow constants, *Phys. Rev. D* **108**, 084006 (2023), arXiv:2309.08071 [gr-qc].
 - [27] C. T. Y. Chung and A. Melatos, Stokes tomography of radio pulsar magnetospheres - I. Linear polarization, *MNRAS* **411**, 2471 (2011), arXiv:1010.2816 [astro-ph.SR].
 - [28] C. T. Y. Chung and A. Melatos, Stokes tomography of radio pulsar magnetospheres - II. Millisecond pulsars, *MNRAS* **415**, 1703 (2011), arXiv:1104.1016 [astro-ph.SR].
 - [29] A. V. Bilous, A. L. Watts, A. K. Harding, T. E. Riley, Z. Arzoumanian, S. Bogdanov, K. C. Gendreau, P. S. Ray, S. Guillot, W. C. G. Ho, and D. Chakrabarty, A NICER View of PSR J0030+0451: Evidence for a Global-scale Multipolar Magnetic Field, *ApJ* **887**, L23 (2019), arXiv:1912.05704 [astro-ph.HE].
 - [30] R. C. R. de Lima, J. G. Coelho, J. P. Pereira, C. V. Rodrigues, and J. A. Rueda, Evidence for a Multipolar Magnetic Field in SGR J1745-2900 from X-Ray Light-curve Analysis, *ApJ* **889**, 165 (2020), arXiv:1912.12336 [astro-ph.SR].
 - [31] B. P. Abbott *et al.*, GW170817: Observation of Gravitational Waves from a Binary Neutron Star Inspiral, *Phys. Rev. Lett.* **119**, 161101 (2017), arXiv:1710.05832 [gr-qc].
 - [32] N. Stergioulas, T. A. Apostolatos, and J. A. Font, Non-linear pulsations in differentially rotating neutron stars: mass-shedding-induced damping and splitting of the fundamental mode, *MNRAS* **352**, 1089 (2004), arXiv:astro-ph/0312648 [astro-ph].
 - [33] K. D. Kokkotas and N. Stergioulas, Gravitational Waves from Compact Sources, in *New Worlds in Astroparticle Physics: Proceedings of the Fifth International Workshop*, edited by A. M. Mourão, M. Pimenta, R. Potting, and P. M. Sá (2006) pp. 25–46, arXiv:gr-qc/0506083 [gr-qc].
 - [34] A. G. Pili, N. Bucciantini, and L. Del Zanna, Axisymmetric equilibrium models for magnetized neutron stars in General Relativity under the Conformally Flat Condition, *MNRAS* **439**, 3541 (2014), arXiv:1401.4308 [astro-ph.HE].
 - [35] C. D. Ott, A. Burrows, T. A. Thompson, E. Livne, and R. Walder, The Spin Periods and Rotational Profiles of Neutron Stars at Birth, *ApJS* **164**, 130 (2006), arXiv:astro-ph/0508462 [astro-ph].
 - [36] D. J. Price and S. Rosswog, Producing Ultrastrong Magnetic Fields in Neutron Star Mergers, *Science* **312**, 719 (2006), arXiv:astro-ph/0603845 [astro-ph].
 - [37] K. Kiuchi, Y. Sekiguchi, K. Kyutoku, M. Shibata, K. Taniguchi, and T. Wada, High resolution magnetohydrodynamic simulation of black hole-neutron star merger: Mass ejection and short gamma ray bursts, *Phys. Rev. D* **92**, 064034 (2015), arXiv:1506.06811 [astro-ph.HE].
 - [38] K. Kiuchi, P. Cerdá-Durán, K. Kyutoku, Y. Sekiguchi, and M. Shibata, Efficient magnetic-field amplification due to the Kelvin-Helmholtz instability in binary neutron star mergers, *Phys. Rev. D* **92**, 124034 (2015), arXiv:1509.09205 [astro-ph.HE].
 - [39] R. Aguilera-Miret, D. Viganò, F. Carrasco, B. Miñano, and C. Palenzuela, Turbulent magnetic-field amplification in the first 10 milliseconds after a binary neutron star merger: Comparing high-resolution and large-eddy simulations, *Phys. Rev. D* **102**, 103006 (2020), arXiv:2009.06669 [gr-qc].
 - [40] M. Hanauske, K. Takami, L. Bovard, L. Rezzolla, J. A. Font, F. Galeazzi, and H. Stöcker, Rotational properties of hypermassive neutron stars from binary mergers, *Phys. Rev. D* **96**, 043004 (2017), arXiv:1611.07152 [gr-qc].
 - [41] N. Andersson and K. D. Kokkotas, Towards gravitational wave asteroseismology, *MNRAS* **299**, 1059 (1998), arXiv:gr-qc/9711088 [gr-qc].
 - [42] S. Yoshida and Y. Eriguchi, A Numerical Study of Normal Modes of Rotating Neutron Star Models by the Cowling Approximation, *ApJ* **515**, 414 (1999), arXiv:astro-ph/9807254 [astro-ph].
 - [43] K. D. Kokkotas, T. A. Apostolatos, and N. Andersson, The inverse problem for pulsating neutron stars: a ‘fingerprint analysis’ for the supranuclear equation of state, *MNRAS* **320**, 307 (2001), arXiv:gr-qc/9901072 [gr-qc].
 - [44] J. A. Font, H. Dimmelmeier, A. Gupta, and N. Stergioulas, Axisymmetric modes of rotating relativistic stars in the Cowling approximation, *MNRAS* **325**, 1463 (2001), arXiv:astro-ph/0012477 [astro-ph].
 - [45] S. Yoshida, L. Rezzolla, S. Karino, and Y. Eriguchi, Frequencies of f-Modes in Differentially Rotating Relativistic Stars and Secular Stability Limits, *ApJ* **568**, L41 (2002), arXiv:gr-qc/0112017 [gr-qc].
 - [46] J. A. Font, T. Goodale, S. Iyer, M. Miller, L. Rezzolla, E. Seidel, N. Stergioulas, W.-M. Suen, and M. Tobias, Three-dimensional numerical general relativistic hydrodynamics. II. Long-term dynamics of single relativistic stars, *Phys. Rev. D* **65**, 084024 (2002), arXiv:gr-qc/0110047 [gr-qc].
 - [47] O. Benhar, V. Ferrari, and L. Gualtieri, Gravitational wave asteroseismology reexamined, *Phys. Rev. D* **70**, 124015 (2004), arXiv:astro-ph/0407529 [astro-ph].
 - [48] S. Yoshida, S. Yoshida, and Y. Eriguchi, R-mode oscillations of rapidly rotating barotropic stars in general relativity: analysis by the relativistic Cowling approximation, *MNRAS* **356**, 217 (2005), arXiv:astro-ph/0406283 [astro-ph].
 - [49] H. Dimmelmeier, N. Stergioulas, and J. A. Font, Non-linear axisymmetric pulsations of rotating relativistic stars in the conformal flatness approximation, *MNRAS* **368**, 1609 (2006), arXiv:astro-ph/0511394 [astro-ph].
 - [50] C. Krüger, E. Gaertig, and K. D. Kokkotas, Oscillations and instabilities of fast and differentially rotating relativistic stars, *Phys. Rev. D* **81**, 084019 (2010), arXiv:0911.2764 [astro-ph.SR].
 - [51] E. Gaertig and K. D. Kokkotas, Gravitational wave asteroseismology with fast rotating neutron stars, *Phys. Rev. D* **83**, 064031 (2011), arXiv:1005.5228 [astro-

- ph.SR].
- [52] D. D. Doneva, E. Gaertig, K. D. Kokkotas, and C. Krüger, Gravitational wave asteroseismology of fast rotating neutron stars with realistic equations of state, *Phys. Rev. D* **88**, 044052 (2013), arXiv:1305.7197 [astro-ph.SR].
 - [53] C. J. Krüger and K. D. Kokkotas, Fast Rotating Relativistic Stars: Spectra and Stability without Approximation, *Phys. Rev. Lett.* **125**, 111106 (2020), arXiv:1910.08370 [gr-qc].
 - [54] A. K. L. Yip, P. Chi-Kit Cheong, and T. G. F. Li, Universal relations for fundamental modes of rotating neutron stars with differential rotations, arXiv e-prints, arXiv:2401.13993 (2024), arXiv:2401.13993 [astro-ph.HE].
 - [55] M. v. Hoven and Y. Levin, Magnetar oscillations – I. Strongly coupled dynamics of the crust and the core, *MNRAS* **410**, 1036 (2010), <https://academic.oup.com/mnras/article-pdf/410/2/1036/3437530/mnras0410-1036.pdf>.
 - [56] N. Messios, D. B. Papadopoulos, and N. Stergioulas, Torsional oscillations of magnetized relativistic stars, *MNRAS* **328**, 1161 (2001), arXiv:astro-ph/0105175 [astro-ph].
 - [57] H. Sotani and K. D. Kokkotas, Alfvén polar oscillations of relativistic stars, *MNRAS* **395**, 1163 (2009), arXiv:0902.1490 [astro-ph.HE].
 - [58] M. Gabler, P. Cerdá-Durán, N. Stergioulas, J. A. Font, and E. Müller, Magnetoelastic oscillations of neutron stars with dipolar magnetic fields, *MNRAS* **421**, 2054 (2012), arXiv:1109.6233 [astro-ph.HE].
 - [59] M. Y. Leung, A. K. L. Yip, P. C.-K. Cheong, and T. G. F. Li, Oscillations of highly magnetized non-rotating neutron stars, *Communications Physics* **5**, 334 (2022), arXiv:2303.05684 [astro-ph.HE].
 - [60] A. K. L. Yip, P. C.-K. Cheong, and T. G. F. Li, Formation of a magnetized hybrid star with a purely toroidal field from phase-transition-induced collapse, *MNRAS* **534**, 3612 (2024), arXiv:2303.16820 [astro-ph.HE].
 - [61] A. K. L. Yip, P. C.-K. Cheong, and T. G. F. Li, Gravitational wave signatures from the phase-transition-induced collapse of a magnetized neutron star, *Phys. Rev. D* **112**, 043035 (2025), arXiv:2305.15181 [astro-ph.HE].
 - [62] S. K. Lander, D. I. Jones, and A. Passamonti, Oscillations of rotating magnetized neutron stars with purely toroidal magnetic fields, *MNRAS* **405**, 318 (2010), arXiv:0912.3480 [astro-ph.SR].
 - [63] S. K. Lander and D. I. Jones, Oscillations and instabilities in neutron stars with poloidal magnetic fields, *MNRAS* **412**, 1730 (2011), arXiv:1010.0614 [astro-ph.SR].
 - [64] P. C.-K. Cheong, L.-M. Lin, and T. G. F. Li, Gmunu: toward multigrid based Einstein field equations solver for general-relativistic hydrodynamics simulations, *Classical and Quantum Gravity* **37**, 145015 (2020), arXiv:2001.05723 [gr-qc].
 - [65] P. C.-K. Cheong, A. T.-L. Lam, H. H.-Y. Ng, and T. G. F. Li, Gmunu: paralleled, grid-adaptive, general-relativistic magnetohydrodynamics in curvilinear geometries in dynamical space-times, *MNRAS* **508**, 2279 (2021), arXiv:2012.07322 [astro-ph.IM].
 - [66] P. C.-K. Cheong, D. Y. T. Pong, A. K. L. Yip, and T. G. F. Li, An Extension of Gmunu: General-relativistic Resistive Magnetohydrodynamics Based on Staggered-meshed Constrained Transport with Elliptic Cleaning, *ApJS* **261**, 22 (2022), arXiv:2110.03732 [astro-ph.IM].
 - [67] V. Paschalidis, W. E. East, F. Pretorius, and S. L. Shapiro, One-arm spiral instability in hypermassive neutron stars formed by dynamical-capture binary neutron star mergers, *Phys. Rev. D* **92**, 121502 (2015), arXiv:1510.03432 [astro-ph.HE].
 - [68] H. H.-Y. Ng, P. C.-K. Cheong, L.-M. Lin, and T. G. F. Li, Gravitational-wave Asteroseismology with f-modes from Neutron Star Binaries at the Merger Phase, *ApJ* **915**, 108 (2021), arXiv:2012.08263 [astro-ph.HE].
 - [69] A. K. L. Yip, M. Y. Leung, P. C.-K. Cheong, and T. G. F. Li, Dynamics and gravitational wave signatures of highly magnetized compact stars, *PoS ICRC2023*, 1518 (2023).
 - [70] P. C.-K. Cheong, F. Foucart, M. D. Duez, A. Ofermans, N. Muhammed, and P. Chawhan, Energy-dependent and Energy-integrated Two-moment General-relativistic Neutrino Transport Simulations of a Hypermassive Neutron Star, *ApJ* **975**, 116 (2024), arXiv:2407.16017 [astro-ph.HE].
 - [71] P. C.-K. Cheong, N. Muhammed, P. Chawhan, M. D. Duez, F. Foucart, L. E. Kidder, H. P. Pfeiffer, and M. A. Scheel, High angular momentum hot differentially rotating equilibrium star evolutions in conformally flat spacetime, *Phys. Rev. D* **110**, 043015 (2024), arXiv:2402.18529 [astro-ph.HE].
 - [72] N. Muhammed, M. D. Duez, P. Chawhan, N. Ghadiri, L. T. Buchman, F. Foucart, P. C.-K. Cheong, L. E. Kidder, H. P. Pfeiffer, and M. A. Scheel, Stability of hypermassive neutron stars with realistic rotation and entropy profiles, *Phys. Rev. D* **110**, 124063 (2024), arXiv:2403.05642 [gr-qc].
 - [73] P. C.-K. Cheong, F. Foucart, H. H.-Y. Ng, A. Ofermans, M. D. Duez, N. Muhammed, and P. Chawhan, Influence of neutrino-electron scattering and neutrino-pair annihilation on hypermassive neutron star, *Phys. Rev. D* **111**, 043036 (2025), arXiv:2410.20681 [astro-ph.HE].
 - [74] P. C.-K. Cheong, A. Tsokaros, M. Ruiz, F. Venturi, J. C. L. Chan, A. K. L. Yip, and K. Uryū, General-relativistic resistive-magnetohydrodynamics simulations of self-consistent magnetized rotating neutron stars, *Phys. Rev. D* **111**, 063030 (2025), arXiv:2409.10508 [astro-ph.HE].
 - [75] R. W. Romani, D. Kandel, A. V. Filippenko, T. G. Brink, and W. Zheng, PSR J0952-0607: The Fastest and Heaviest Known Galactic Neutron Star, *ApJ* **934**, L17 (2022), arXiv:2207.05124 [astro-ph.HE].
 - [76] N. Bucciantini and L. Del Zanna, General relativistic magnetohydrodynamics in axisymmetric dynamical spacetimes: the X-ECHO code, *A&A* **528**, A101 (2011), arXiv:1010.3532 [astro-ph.IM].
 - [77] A. G. Pili, N. Bucciantini, and L. Del Zanna, General relativistic neutron stars with twisted magnetosphere, *MNRAS* **447**, 2821 (2015), arXiv:1412.4036 [astro-ph.HE].
 - [78] A. G. Pili, N. Bucciantini, and L. Del Zanna, General relativistic models for rotating magnetized neutron stars in conformally flat space-time, *MNRAS* **470**, 2469 (2017), arXiv:1705.03795 [astro-ph.HE].
 - [79] J. Soldateschi, N. Bucciantini, and L. Del Zanna, Axisymmetric equilibrium models for magnetised neutron

- stars in scalar-tensor theories, *A&A* **640**, A44 (2020), arXiv:2005.12758 [astro-ph.HE].
- [80] M. Herbrink and K. D. Kokkotas, Stability analysis of magnetized neutron stars - a semi-analytic approach, *MNRAS* **466**, 1330 (2017), arXiv:1511.04290 [astro-ph.SR].
 - [81] J. Antoniadis, P. C. C. Freire, N. Wex, T. M. Tauris, R. S. Lynch, M. H. van Kerkwijk, M. Kramer, C. Bassa, V. S. Dhillon, T. Driebe, J. W. T. Hessels, V. M. Kaspi, V. I. Kondratiev, N. Langer, T. R. Marsh, M. A. McLaughlin, T. T. Pennucci, S. M. Ransom, I. H. Stairs, J. van Leeuwen, J. P. W. Verbiest, and D. G. Whelan, A Massive Pulsar in a Compact Relativistic Binary, *Science* **340**, 448 (2013), arXiv:1304.6875 [astro-ph.HE].
 - [82] E. Fonseca, H. T. Cromartie, T. T. Pennucci, P. S. Ray, A. Y. Kirichenko, S. M. Ransom, P. B. Demorest, I. H. Stairs, Z. Arzoumanian, L. Guillemot, A. Parthasarathy, M. Kerr, I. Cognard, P. T. Baker, H. Blumer, P. R. Brook, M. DeCesar, T. Dolch, F. A. Dong, E. C. Ferrara, W. Fiore, N. Garver-Daniels, D. C. Good, R. Jennings, M. L. Jones, V. M. Kaspi, M. T. Lam, D. R. Lorimer, J. Luo, A. McEwen, J. W. McKee, M. A. McLaughlin, N. McMann, B. W. Meyers, A. Naidu, C. Ng, D. J. Nice, N. Pol, H. A. Radovan, B. Shapiro-Albert, C. M. Tan, S. P. Tendulkar, J. K. Swiggum, H. M. Wahl, and W. W. Zhu, Refined Mass and Geometric Measurements of the High-mass PSR J0740+6620, *ApJ* **915**, L12 (2021), arXiv:2104.00880 [astro-ph.HE].
 - [83] G. Tóth and D. Odstrčil, Comparison of Some Flux Corrected Transport and Total Variation Diminishing Numerical Schemes for Hydrodynamic and Magnetohydrodynamic Problems, *Journal of Computational Physics* **128**, 82 (1996).
 - [84] P. Colella and P. R. Woodward, The Piecewise Parabolic Method (PPM) for Gas-Dynamical Simulations, *Journal of Computational Physics* **54**, 174 (1984).
 - [85] C.-W. Shu and S. Osher, Efficient Implementation of Essentially Non-oscillatory Shock-Capturing Schemes, *Journal of Computational Physics* **77**, 439 (1988).
 - [86] K. Uryū, A. Tsokaros, L. Baiotti, F. Galeazzi, K. Taniguchi, and S. Yoshida, Modeling differential rotations of compact stars in equilibriums, *Phys. Rev. D* **96**, 103011 (2017), arXiv:1709.02643 [astro-ph.HE].
 - [87] P. Iosif and N. Stergioulas, Models of binary neutron star remnants with tabulated equations of state, *MNRAS* **510**, 2948 (2022), arXiv:2104.13672 [astro-ph.HE].
 - [88] M. Cassing and L. Rezzolla, Realistic models of general-relativistic differentially rotating stars, *MNRAS* **532**, 945 (2024), arXiv:2405.06609 [gr-qc].
 - [89] H. Komatsu, Y. Eriguchi, and I. Hachisu, Rapidly rotating general relativistic stars. I - Numerical method and its application to uniformly rotating polytropes, *MNRAS* **237**, 355 (1989).
 - [90] H. Komatsu, Y. Eriguchi, and I. Hachisu, Rapidly rotating general relativistic stars. II - Differentially rotating polytropes, *MNRAS* **239**, 153 (1989).
 - [91] T. W. Baumgarte, S. L. Shapiro, and M. Shibata, On the Maximum Mass of Differentially Rotating Neutron Stars, *ApJ* **528**, L29 (2000), arXiv:astro-ph/9910565 [astro-ph].
 - [92] I. A. Morrison, T. W. Baumgarte, and S. L. Shapiro, Effect of Differential Rotation on the Maximum Mass of Neutron Stars: Realistic Nuclear Equations of State, *ApJ* **610**, 941 (2004), arXiv:astro-ph/0401581 [astro-ph].
 - [93] J. D. Kaplan, C. D. Ott, E. P. O'Connor, K. Kiuchi, L. Roberts, and M. Duez, The Influence of Thermal Pressure on Equilibrium Models of Hypermassive Neutron Star Merger Remnants, *ApJ* **790**, 19 (2014), arXiv:1306.4034 [astro-ph.HE].
 - [94] L. Villain, J. A. Pons, P. Cerdá-Durán, and E. Gourgoulhon, Evolutionary sequences of rotating protoneutron stars, *A&A* **418**, 283 (2004), arXiv:astro-ph/0310875 [astro-ph].
 - [95] LIGO Scientific Collaboration *et al.*, Advanced LIGO, Classical and Quantum Gravity **32**, 074001 (2015), arXiv:1411.4547 [gr-qc].
 - [96] F. Acernese *et al.*, Advanced Virgo: a second-generation interferometric gravitational wave detector, Classical and Quantum Gravity **32**, 024001 (2015), arXiv:1408.3978 [gr-qc].
 - [97] K. Somiya, Detector configuration of KAGRA-the Japanese cryogenic gravitational-wave detector, Classical and Quantum Gravity **29**, 124007 (2012), arXiv:1111.7185 [gr-qc].
 - [98] Y. Aso, Y. Michimura, K. Somiya, M. Ando, O. Miyakawa, T. Sekiguchi, D. Tatsumi, and H. Yamamoto, Interferometer design of the KAGRA gravitational wave detector, *Phys. Rev. D* **88**, 043007 (2013), arXiv:1306.6747 [gr-qc].
 - [99] M. Punturo *et al.*, The Einstein Telescope: a third-generation gravitational wave observatory, Classical and Quantum Gravity **27**, 194002 (2010).
 - [100] B. P. Abbott *et al.*, Exploring the sensitivity of next generation gravitational wave detectors, Classical and Quantum Gravity **34**, 044001 (2017), arXiv:1607.08697 [astro-ph.IM].
 - [101] D. Reitze, LIGO Laboratory: California Institute of Technology, LIGO Laboratory: Massachusetts Institute of Technology, LIGO Hanford Observatory, and LIGO Livingston Observatory, The US Program in Ground-Based Gravitational Wave Science: Contribution from the LIGO Laboratory, *BAAS* **51**, 141 (2019), arXiv:1903.04615 [astro-ph.IM].
 - [102] D. Reitze, R. X. Adhikari, S. Ballmer, B. Barish, L. Barsotti, G. Billingsley, D. A. Brown, Y. Chen, D. Coyne, R. Eisenstein, M. Evans, P. Fritschel, E. D. Hall, A. Lazzarini, G. Lovelace, J. Read, B. S. Sathyaprakash, D. Shoemaker, J. Smith, C. Torrie, S. Vitale, R. Weiss, C. Wipf, and M. Zucker, Cosmic Explorer: The U.S. Contribution to Gravitational-Wave Astronomy beyond LIGO, in *Bulletin of the American Astronomical Society*, Vol. 51 (2019) p. 35, arXiv:1907.04833 [astro-ph.IM].
 - [103] A. Puecher, T. Dietrich, K. W. Tsang, C. Kalaghatgi, S. Roy, Y. Setyawati, and C. Van Den Broeck, Unraveling information about supranuclear-dense matter from the complete binary neutron star coalescence process using future gravitational-wave detector networks, *Phys. Rev. D* **107**, 124009 (2023), arXiv:2210.09259 [gr-qc].
 - [104] G. Camelió, T. Dietrich, S. Rosswog, and B. Haskell, Axisymmetric models for neutron star merger remnants with realistic thermal and rotational profiles, *Phys. Rev. D* **103**, 063014 (2021), arXiv:2011.10557 [astro-ph.HE].